Received: 12 August 2021 | Accepted: 14 September 2021 | Published online: 23 October 2021

DOI: 10.1111/opo.12903

OPO THE COLLEGE OF OPTOMETRISTS

ORIGINAL ARTICLE

Retinal defocus in myopes wearing dual-focus zonal contact lenses

Neeraj K Singh | **Dawn Meyer** | **Matt Jaskulski** | **Pete Kollbaum**

School of Optometry, Indiana University, Bloomington, Indiana, USA

Correspondence
Neeraj K Singh, School of Optometry, Indiana University, Bloomington, Indiana, USA.
Email: neesingh@iu.edu

Funding information
Partially supported by CooperVision Inc., CA (PK).

Abstract

Purpose: To evaluate the refractive impact of dual-focus (DF) myopia control contact lenses (CLs) on accommodating young myopic adults.

Methods: Phase 1: accommodative accuracy was assessed in 40 myopic participants. Phase 2: a subset of four subjects who demonstrated accurate accommodation and six who chronically underaccommodated were fitted with single vision (SV, Proclear 1 day) and centre-distance DF myopia control CLs (MiSight 1 day) with approximately +2.00 D of additional power in two surrounding annular zones. While binocularly viewing high contrast characters at 4.00, 1.00, 0.50, 0.33, 0.25 and 0.20 m, aberrometry data were captured across the central ±30° of the horizontal retina. Local refractive errors were pooled for each area of the pupil covered by the central distance or first annular defocus zone of the DF CLs.

Results: In the "good" accommodator group fitted with SV CLs, accommodative lags were generally absent except at the closest viewing distance (mean errors: −0.09 ± 0.22 D, −0.12 ± 0.26 D, −0.05 ± 0.37 D and +0.38 ± 0.54 D for −2.00, −3.00, −4.00 and −5.00 D target vergences, respectively) but significantly larger in the "poor" accommodating participants (+0.81 ± 0.21 D, +0.97 ± 0.27 D, +1.18 ± 0.39 D, +1.47 ± 0.55 D). For most viewing distances, hyperopic defocus observed in the region of the pupil covered by the first annular zone was replaced with myopic defocus when fitted with the DF CLs. Myopic defocus created by the first annular region was present across the central 30° of the retina.

Conclusions: Some young adult myopes chronically experience high levels of hyperopic defocus when viewing near targets, which was replaced by myopic defocus in the annular part of the pupil covered by the treatment zones when fitted with a centre-distance myopia control DF CL.

KEYWORDS
accommodation, contact lenses, dual-focus, myopia, optical aberrations, peripheral refraction, retinal defocus

INTRODUCTION

The correction of myopia traditionally employs spectacles, contact lenses (CLs) or corneal reshaping using orthokeratology or refractive surgery. These approaches all employ refractive optical principles to make distant targets conjugate with the fovea in the unaccommodated eye.[1] However, when the foveal image is focused in myopic eyes or those destined to become myopic,[2,3] hyperopic defocus can exist in the extrafoveal regions. Importantly, studies of infant monkeys suggest that hyperopic defocus, even when absent from the central 10° of the retina accelerated eye growth, ultimately generating myopic eyes.[4] The presence of myopic defocus can slow eye growth,[5] and can prevent growth that would otherwise have been caused by the simultaneous presence of hyperopic defocus.[6]

The term "hyperopic defocus" describes the situation where the image plane lies posterior to the photoreceptor plane, which can occur if the eye is too short for its optical power ("hyperopia"), as is the case in the typical infant eye.[7] Eyes also routinely establish retinal conjugate planes more posterior than ideal for proximal stimuli ("accommodative lag"[8,9]), thereby placing the image plane behind the retina. In the presence of hyperopic defocus, retinal image focus can be achieved by either moving the image plane forward by accommodation,[10] the use of plus-power ophthalmic lenses or by moving the retina back with eye growth.[6] Eye growth in hyperopic infant eyes typically results in approximate emmetropia, a process called "emmetropization".[2] However, eye growth to match the image and retinal planes due to habitual near viewing[11–14] and accommodative lag[8] will result in an eye that is too long for distance viewing, i.e., the development of "myopia".[15]

Dual-focus (DF) CLs employ regions of added plus power designed to introduce myopic defocus as a way of controlling the effects of any co-occurring hyperopic defocus,[6] and have been shown to slow the rate of myopia by more than 50% (myopia progression was reduced by 0.73 D in the treated cohort) in children.[16] However, the efficacy of such plus power containing treatments often varies from child to child.[16,17] One possible explanation is that some eyes experience varying amounts of hyperopic defocus, and therefore different degrees of induced myopic defocus, in part due to their accommodative response when fitted with myopia control DF CLs.[18] The purpose of the present study was to examine the impact of a CL employing DF optics on the presence of hyperopic defocus across the central 30° of the horizontal retina in young adults who either accommodated accurately or who had larger than average lags of accommodation.

Key points

- At typical near reading distances, accommodative lags measured in the pupil centre remained when fitted with centre-distance dual-focus contact lenses, indicating that accommodative behaviour is dominated by the central zone optics.
- Hyperopic defocus due to accommodative lags was replaced with myopic defocus by the annular zones of the dual-focus contact lenses that contained an additional +2.00 D power.
- Individuals with higher accommodative lags experienced less myopic defocus in the annular zones. The tested dual-focus myopia control lens was able to replace hyperopic with myopic defocus across the central 30° of the retina.

METHODS

In Phase 1 of this study, the accommodative responses of 40 young myopic adults wearing single vision (SV) CLs was obtained. From these responses, two subsets of participants were selected to complete a second study phase: those participants who had accommodative responses within either the upper or lower response quartiles, and those with the least or greatest accommodative lags. For simplicity, these participants are termed "good" (least accommodative lag) and "poor" (most accommodative lag) accommodating participants when referenced below. Foveal and off-axis refractive states were then measured in these subsamples while they were wearing DF CL that corrected their distance refractive errors. The study protocol followed the tenets of the Declaration of Helsinki and was approved by the Indiana University research ethics committee. Written informed consent was obtained from each participant before participating in the study.

Participants

Forty young adult (Mean ± SD age; 21.85 ± 1.52 years), non-CL wearing, myopic participants were recruited by word of mouth, from recruitment databases and using an advertisement circulated via email and social media platforms. Participants were screened with a routine eye examination to determine subjective refraction, visual acuity and general ocular health. Myopic participants (spherical equivalent refraction (SER) < −0.50 D)[19] with good visual acuity (0.00 logMAR or better), no manifest strabismus or amblyopia and no history of refractive surgery or ocular disease were recruited. Mean ± SD SER was −3.33 ± 1.40 D (range −0.75 to −6.50 D). From the overall sample, 10 participants (four with small [Mean ± SD SER = −3.69 ± 1.38] and six with larger [Mean ± SD SER = −3.33 ± 1.32] accommodative lags) who were available and willing to participate in subsequent testing were fitted with DF CLs (MiSight 1 day, omafilcon A, CooperVision, coopervision.com).

Contact lenses

The spherical SV CLs (Proclear 1-Day, omafilcon A, CooperVision, coopervision.com) had a base curve of 8.70 mm and diameter of 14.20 mm. The DF CLs (MiSight 1 day) had a base curve of 8.70 mm and diameter of 14.20 mm. The CL wavefront error and power maps (*Figure 1*) were measured *ex-vivo* using a previously validated[20] single-pass Shack–Hartmann wavefront sensor with a sampling resolution of 104 microns (ClearWave, Lumetrics, lumetrics.com). Eyes were fitted with lenses to optimize monocular distance vision (maximum plus or minimum minus correction).

The DF CLs consisted of four alternating distance and near zones with measured radii of approximately 1.65, 2.40, 3.40 and 4.40 mm, respectively, from the innermost to the outermost rings (*Figure 1*, right panels), which is consistent with previous reports.[21] Zones 1 and 3 were distance vision correcting zones and zones 2 and 4 were "defocus" or "treatment zones" with a designed additional +2.00 D. The spherical aberration (C_4^0) for this measured DF CL (with nominal distance power of –1.25 D) within the central distance correction zone (radius = 1.65 mm) was 0.01 microns. The SV CL with nominal power of –1.00 D included a low level (–0.16 microns) of negative C_4^0 over a 7-mm pupil diameter. The mean ± SD C_4^0 for the SV CL sphere powers ranging from –1.00 to –6.00 D used in this study was –0.30 ± 0.13 microns.

Measurement procedures

By inserting a 45° tilted infrared reflecting beam splitter into the measurement path, a validated[22] high sampling density (41-μm samples in the pupil plane) double-pass pyramidal wavefront sensing aberrometer (Osiris, Costruzione Strumenti Oftalmici,csoitalia.it) was adapted to assess the refractive state of the right eyes during binocular viewing. Fixated stimuli were positioned at 4.00, 1.00, 0.50, 0.33, 0.25 and 0.20 m (corresponding to target vergences of –0.25, –1.00, –2.00, –3.00, –4.00 and –5.00 D) from the eye. Measurements were taken at the fovea and at ±10, 20 and 30° across the central retina. Eye stability was aided by a chin- and forehead rest. On-axis (foveal) measurements were obtained by aligning the fixation target with the instrument measurement axis.

Participants binocularly viewed a high spatial bandwidth stimulus. At all near viewing distances, this consisted of a changing sequence of 0.30 logMAR equivalent letter characters displayed on an iPhone 6 (Apple, apple.com). At 4.00 m, subjects viewed the 0.30 logMAR line on an illuminated Early Treatment Diabetic Retinopathy

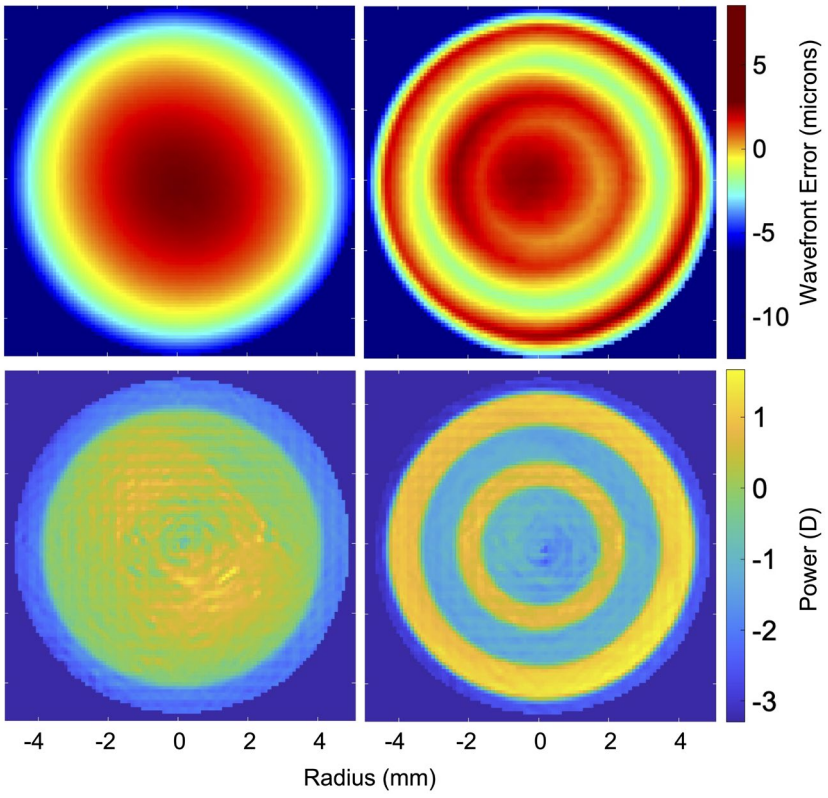

FIGURE 1 Colour maps of ex-vivo measured wavefront error (top panels, microns) and power (bottom panels, dioptres) of the single vision (SV) (left panels) and dual-focus (DF) (right panels) contact lenses (CLs) across a 10.00 mm measurement diameter with nominal distance powers of –1.00 and –1.25 D, respectively. Map coordinates are in mm. The measured optical zones of the SV and DF CLs have diameters of approximately 8.00 and 9.00 mm, respectively

Study (ETDRS) chart. During the measurements, participants were instructed to "keep the target single and as clear as possible". A "sham" task of having participants press a key on the keyboard when they saw a particular letter was employed to aid attention. Off-axis measurements were achieved by rotating a mechanical arm holding the iPhone and fixation target with its centre of rotation located directly above the participant's right eye. Eye fixation to the right placed the measurement axis into the nasal visual field, and thus measures refractive state for the temporal retina, and vice versa. Fixation locations were randomized for off-axis measurements. Three single aberrometry acquisitions were obtained for each fixation target location.

Data analysis

Wavefront data for the full natural pupil were exported and processed using customised software (Indiana Wavefront Analyzer [IWA])[23] implemented in MATLAB (Mathworks, mathworks.com). Elliptical analysis zones were used when analysing off-axis data.[24,25] Local integration of the slope data provided zonally reconstructed wavefronts avoiding Zernike fitting.[26] Radial slope divided by the distance from the pupil centre or CL centre yielded the local wavefront radial vergence, or local refractive state when measuring output from the eye.[27] These measures capture local refractive errors generated by uncorrected sphere, astigmatism, accommodative errors and higher order aberrations. Dioptre histograms quantifying the number of samples (reflecting local area) corresponding to a dioptre level in 0.125 D increments were derived from these local sagittal power maps. First, the on-axis refractive state of all 40 eyes was quantified as the aberrometer-measured average refractive state within the central 4.00 mm of the pupil while participants viewed the 4.00 m target.[28] In these distance-corrected eyes, differences between the measured local refractive state and the target vergence (refractive state - target vergence) indicated retinal image defocus due to accommodative error. Accommodative lead (myopic defocus) and lag (hyperopic defocus) were represented using negative and positive signs, respectively.

Lens position relative to the pupil centre of the DF zonal CLs was determined by identifying the boundary between the central and first annular zones, and the first and second annular zones from the vergence maps (*Figure 2*, upper panels). Refractive state was quantified as the average within each of the central and first annular treatment zones. In some instances, due to lens decentration the full annular zone was not visible, but any available data within the zones was utilized. For comparison, refractive state data were also collated from the same DF equivalent geographic regions within the pupil when assessing SV lens data (*Figure 2*, lower panels), which allowed the same ocular optics to be included when comparing both lenses.

RESULTS

During the initial screening of 40 participants (*Figure 3*), accommodative lags at near viewing distances (0.50 m–0.20 m) were common (94% of all measurements) with a mean ± SD of +0.34 ± 0.40 D, +0.37 ± 0.44 D, +0.52 ± 0.58 D and +0.71 ± 0.60 D, respectively, for −2.00, −3.00, −4.00 and −5.00 D target vergences. Accommodative errors for the 40 participants wearing the SV CLs at each target distance were highly correlated within a participant, indicating that accommodative lags were habitually present in some participants at all near distances. Pairwise comparisons of lags for target vergences −2.00 and −3.00, −3.00 and −4.00 and −4.00 and −5.00 D produced respective r^2 values of 0.86, 0.75 and 0.87.

From the 40 participants who were originally screened, four were selected from the lower quartile of the accommodative response distribution exhibiting the least accommodative lag (red lines and symbols in *Figure 3*, termed "good" accommodating participants), and six from the upper quartile exhibiting habitual under-accommodion (blue symbols and lines in *Figure 3*, termed "poor" accommodating participants). The mean ± SD accommodative error (lag) of the "good" accommodating participants was −0.09 ± 0.22 D, −0.12 ± 0.26 D, −0.05 ± 0.37 D and +0.38 ± 0.54 D, respectively, for −2.00, −3.00, −4.00 and −5.00 D target vergences, while for the "poor" accommodating participants the mean ± SD accommodative errors were +0.81 ± 0.21 D, +0.97 ± 0.27 D, +1.18 ± 0.39 D and +1.47 ± 0.55 D, respectively, for the −2.00, −3.00, −4.00 and −5.00 D target vergences; statistically larger than those observed in the good accommodators ($p < 0.002$, paired *t*-test).

A representative series of individual accommodative error maps (measured refractive state - target vergence at each location in the pupil) of one "poor" accommodator wearing a DF lens are shown in *Figure 4*. In the on-axis examples (top series of maps), the DF optics of the CL dominate the defocus pattern with the blur ring. The gradual shift toward yellow colours at near distances reveals increasing accommodative lags. When measured off-axis (bottom series of maps), the axial separation of the CL optics and the eye's entrance pupil causes the parallax shift of the CL centre, introducing more peripheral CL optics in front of the pupil.[29–31] The off-axis optics in combination with parallax introduce more complex defocus patterns across the pupil due to oblique astigmatism and coma associated with off-axis optics.[32,33]

The resultant average defocus within the central optical zone and first annular treatment zone is plotted for on-axis measurements in the left panels of *Figure 5*. The good accommodator group (top-left panel) experienced little defocus foveally with the SV CLs, only revealing hyperopic defocus in the equivalent first annular region at the nearest distances. When viewing with the DF lens, on-axis defocus within the central zone of the good accommodating eyes was approximately the same as observed with the SV lenses. This similarity suggests that good accommodating

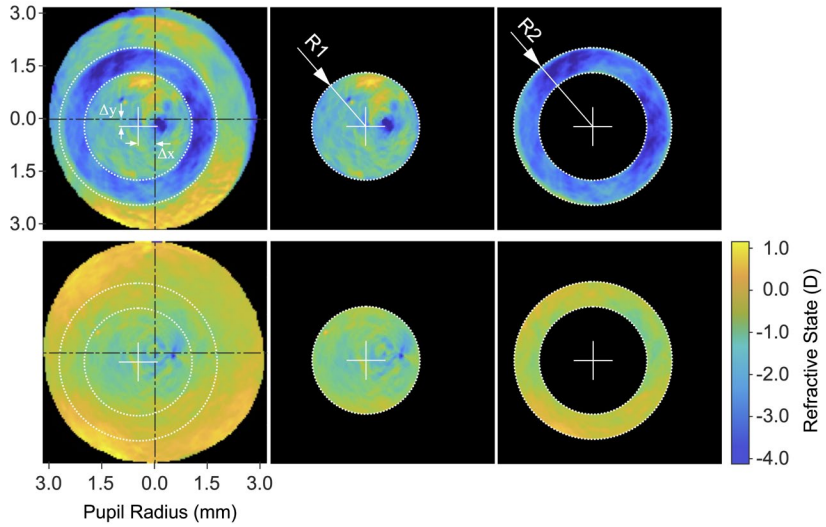

FIGURE 2 Examples of zone-wise analysis methods. Refractive state was quantified as the average dioptric value within the available regions of the central and first annular zone of dual-focus lens (top panels). Equivalent pupil regions were then used to analyse the same regions on the single vision contact lens data (bottom panels)

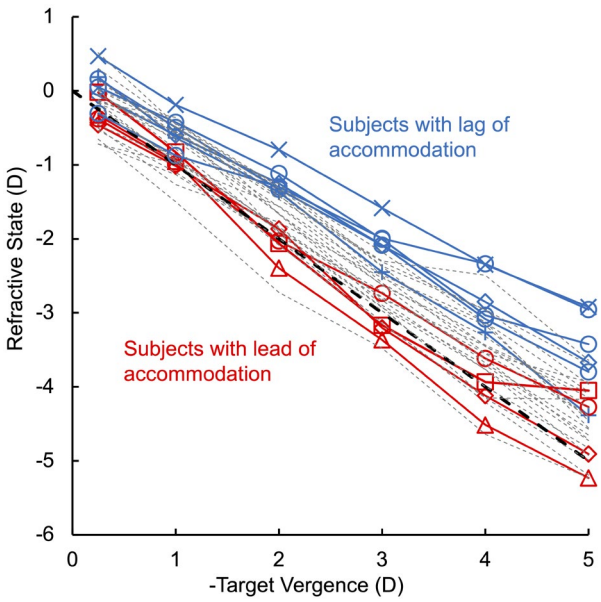

FIGURE 3 Refractive state (mean of three repeat measurements) of 40 participants plotted as a function of target vergence. A sub-sampling of participants with the lowest accommodative lags (red, "good" accommodating participants) and highest accommodative lags (blue, "poor" accommodating participants) were selected for full on- and off-axis testing of both the single vision and dual-focus contact lenses

participants accommodate to focus rays from the central optical region of the pupil, regardless of whether they are fitted with SV or DF CLs.

Because of the increasing negative spherical aberration associated with accommodation,[34,35] even the good accommodating participants experienced some hyperopic defocus in the first annular region (radii 1.65–2.40 mm) when fitted with SV CLs (mean = +0.10 D, +0.10 D, +0.24 D and +0.50 D, respectively, for target vergences of −2.00, −3.00, −4.00 and −5.00 D). However, because of the +2.00 D defocus power in the annulus of the DF lens, the same eyes experienced significant myopic defocus (mean = −1.22, −1.30, −1.29 and −1.14 D, respectively, for target vergences of −2.00, −3.00, −4.00 and −5.00 D). The magnitude of myopic defocus in the first annular zone of the DF lens when on the eye was less than the +2.00 D nominal defocus power (*Figure 1*) stated in the lens design, because ocular negative spherical aberration is added to the plus-power within the annular zone, and a small impact of the narrow transition zone between the central zone and first annual treatment zone.[36]

The on-axis data for the poor accommodating eyes (bottom-left panel, *Figure 5*) fitted with SV CLs also revealed increasing levels of hyperopic defocus at near within the equivalent first annular zone (mean = +0.92, +1.26, +1.41 and +1.87 D, respectively, for target vergences of −2.00, −3.00, −4.00 and −5.00 D), which changed to myopic defocus of −0.85, −0.79, −0.63 and −0.30 D when viewing with the DF CLs.

Average off-axis defocus is plotted (*Figure 5*) as a function of retinal eccentricity while participants viewed fixation stimuli at −1.00 and −4.00 D target vergences (middle and right panels, respectively). At a target vergence of −1.00 D, the good accommodating participants had a well-focused image across most of the 30° of the central retina with the SV lens for both equivalent central and annular zones. There was a clear hyperopic shift at 30° in the temporal retina. The poor accommodating eyes had fairly similar, well-focused images across the central 30° with the SV lenses. At target vergence of −1.00 D, the central zone results remained similar to those of the SV lenses while the defocus zone in the DF lens was able to produce myopic defocus at all eccentricities for both good and poor accommodating eyes. Similar patterns are present in the −4.00 D target vergence data, with a hyperopic shift reflecting the

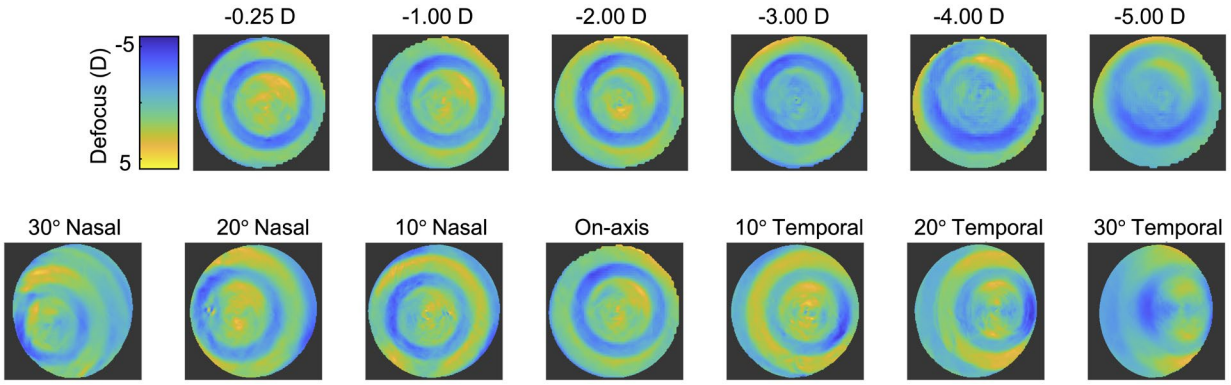

FIGURE 4 Example accommodative error (refractive state – target vergence) maps of one participant (poor accommodator) wearing the dual-focus zonal contact lens for on- (top panels) and off-axis (bottom panels) viewing conditions. Target vergence for the on-axis foveal measurements ranged from −0.25 to −5.00 D (top row), and off-axis retinal eccentricities ranged from 30° nasal to 30° temporal (bottom panels). Off-axis data was collected while viewing a target at 1.00 m. Maps have a fixed size and contain defocus data for the full pupil. Because pupil size varies with viewing distance, the maps at higher target vergences show data across a smaller pupil, and therefore, the central zone, which has a fixed size in the lens, covers a larger proportion of these smaller pupils

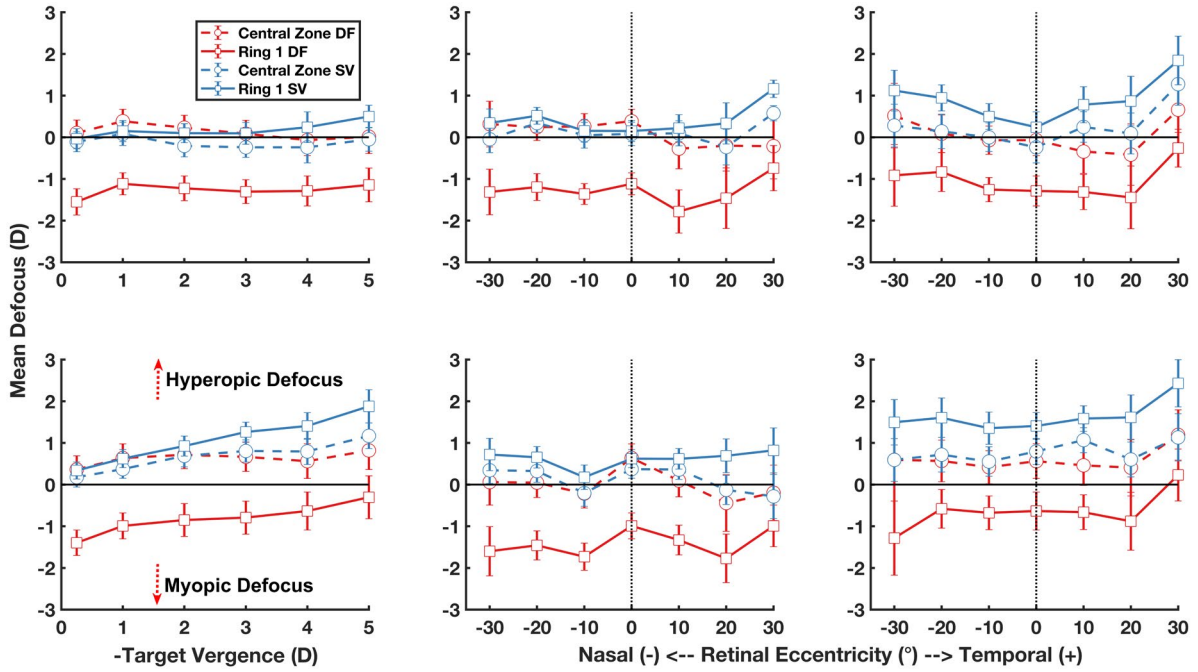

FIGURE 5 Mean defocus as a function of negative target vergence (left panels), and as a function of nasal (negative) and temporal (positive) retinal eccentricity for −1.00 D (middle panels) and −4.00 D (right panels) target vergences. Mean and standard error are plotted for the central distance correction zone (dotted lines) and first annular treatment zone (solid lines) for dual-focus (DF; red lines) and equivalent zones for single vision (SV; blue lines) contact lenses. Top panels represent data from the good accommodating participants while the bottom panels are for poor accommodating participants. Error bars indicate standard error of the mean

generally present accommodative lags for this near viewing distance. The elevated ocular negative spherical aberration at this target vergence contributed a hyperopic shift in the annular zone data, resulting in significant hyperopia when viewing with the SV lens, especially in the poor accommodators in the temporal retina. Myopic defocus created by the annular treatment zone of the DF lenses was present over most of the central retina, but often absent at 30° in the temporal retina when viewing with the DF lens, especially at the near viewing distance in the poor accommodating eyes.

One of the goals of DF optics is to reduce chronic exposure to hyperopic defocus (due to accommodative lags) and replace this with significant myopic defocus as a signal to slow eye growth. The impact of this strategy was examined for the full natural pupil by assessing the proportion of light within the retinal image that was either hyperopically or myopically defocused. Myopia was

defined as SER ≤ −0.50 D,[19] hyperopia ≥ 0.75 D,[37] and emmetropia in between these two refractive zones.[38] *Figure 6* plots the proportion of myopic (x-axis) and hyperopic (y-axis) defocus for each of the good (top row) and poor (bottom row) accommodating participants fitted with SV (blue) and DF (red) CLs for on-axis (foveal) data. Each subplot shows data for each of the target vergences. Data close to the origin indicate that most of the pupil area contributed (emmetropic) focused light, whereas data along the $Y = -X$ line indicate that there is no focused light. Data toward the bottom right indicate more myopic than hyperopic defocus, and conversely data toward the top-left of each panel indicate a predominance of hyperopic defocus. The SV data (blue symbols) clearly distinguishes the good (top row) from poor (bottom row) accommodating participants. In particular, notice that the poor accommodating participants have a larger majority of hyperopically defocused light, which approached 100% at near distances. However, with SV CLs, good accommodating participants experienced a majority of focused light at distance, switching to a lessor majority of hyperopic defocus at the closest distances. The DF CLs, however, successfully provided a mix of focused and myopically defocused light for the good accommodating participants at all viewing distances. The DF CLs also successfully prevented hyperopic defocus from becoming dominant in the poor accommodating participants.

Proportions of focused (blue) and myopically (red) or hyperopically (black) defocused light in the retinal image for each location sampled across the central 30° of the horizontal retina are plotted in *Figures 7* and *8* for the −1.00 and −4.00 D target vergences, respectively. Hyperopic defocus (black symbols) is less dominant in the good (G) than the poor (P) accommodating groups, but significant in both groups fitted with SV CLs when viewing the −4.00 D stimulus (top panels, *Figure 8*). Introduction of the DF optic increased the proportion of myopic defocus in all cases (red symbols, bottom panels), becoming dominant for −1.00 D target vergence, and generally matching the hyperpic proportions for the −4.00 D target vergence.

DISCUSSION

Evaluation of the accommodative responses of 40 young myopic SV-wearing participants revealed significant between-participant differences in accommodative accuracy that were maintained across a wide range of viewing distances. However, between-participant differences became most exaggerated at the nearest target distances. Individuals in the poor accommodating group experienced habitual hyperopic defocus at all near distances, whereas those in the good accommodating group achieved approximate focus at all but the closest distances.

When fitted with DF CLs, individuals in both the good and poor accommodating subsets accommodated such that the defocus generated by the central zone of the DF CLs mirrored that generated over the same pupil area with SV CLs. These results align with previous results that indicated no large effect of DF optics on the accommodative behaviour of young adults.[18,39–41] These results also emphasise that the accommodative behaviour of myopic participants in this study was dominated by the central zone optics when fitted with DF CLs, importantly resulting in myopic defocus generated by the annular defocus zone. In agreement with expectations from previous results, the nominal +2.00 D defocus in the annular "treatment zone"[16] of the DF CLs used in this study was, on average, sufficient to generate myopic defocus even in the presence of the negative spherical aberration generated during accommodation,[34,35,42] but some of the poor accommodators experienced significant

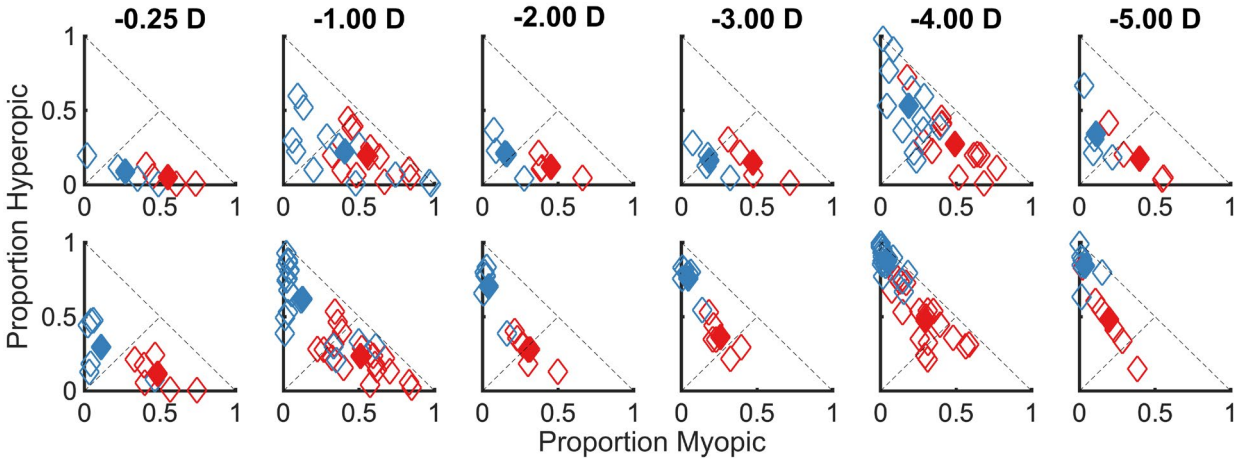

FIGURE 6 Proportion of the full pupil contributing hyperopically defocused (*y*-axis), and myopically defocused (*x*-axis) light to the retinal image for the good accommodating (top panels) and poor accommodating (bottom panels) cohorts. Filled symbols represent the group-mean, whereas open symbols indicate individual eye means of three repeated measurements. Single vision and dual-focus contact lens data are shown in blue and red, respectively

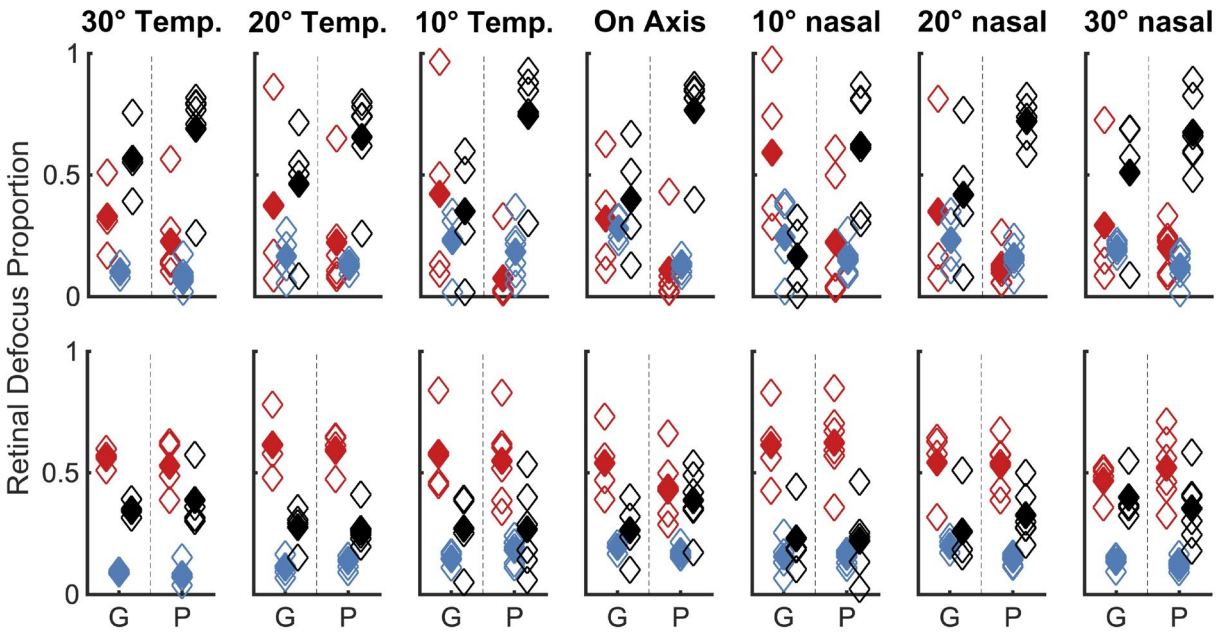

FIGURE 7 The proportion of myopic (red), hyperopic (black) defocus and focused light (blue) present at each retinal eccentricity with a −1.00 D target vergence. The top and bottom panels show data for eyes fitted with single vision and dual-focus contact lens, respectively. Left and right sub-panels show data for the good "G" and poor "P" accommodating groups, respectively. Filled symbols represent group-mean whereas open symbols indicate individual eye means. There is overlay of some coincident individual participant data points

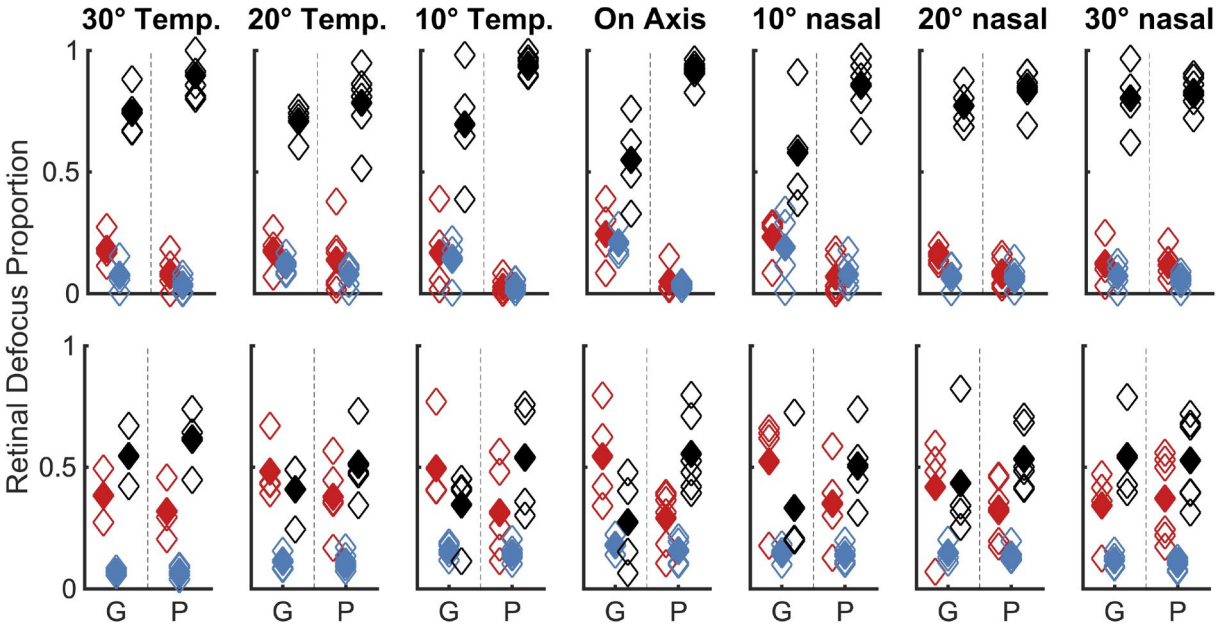

FIGURE 8 The proportion of myopic (red), hyperopic (black) defocus and focused light (blue) present at each retinal eccentricity with a −4.00 D target vergence. The top and bottom panels show data for eyes fitted with single vision and dual-focus contact lens, respectively. Left and right sub-panels show data for the good "G" and poor "P" accommodating groups, respectively. Filled symbols represent group-mean whereas open symbols indicate individual eye means. There is overlay of some coincident individual participant data points

amounts of foveal hyperopic defocus at the nearest viewing distances (*Figures 5* and *6*). These results reveal that DF zonal CL designs with +2.00 D defocus powers can be used to ensure reduced hyperopic defocus and the introduction of significant amounts of myopic defocus across the central horizontal retina for all tested subjects at most viewing distances, as the treatment strategy indicates.[16]

In comparing the current results to previous reports, it is important to highlight some key methodological details. A few studies reporting peripheral refraction and accommodation of either the eye alone or an eye wearing SV CLs, measured mean SER or defocus calculated directly from Zernike coefficients of the entire pupil, and reported that accommodation did not consistently influence the relative off-axis refractions (hyperopic or myopic shift).[43–45] Alternatively, others have noted that relative peripheral refraction tended to become more myopic with accommodation.[46,47] Studies[48–50] reporting off-axis refraction with multifocal CLs have observed similar mean SER from autorefractometers or Zernike derived measures of defocus from aberrometers. Results of these studies of multifocal CLs have also been variable with some finding a myopic shift outside the fovea[48] while others reported a relative hyperopic shift.[50]

Integrating data to arrive at a single measure of SER in eyes fitted with multifocal CLs is dramatically affected by analysis diameter[49] and location[18] of the integration area. For example, minimum root mean square (minRMS) measurements of refractive state will make the eye appear hyperopic relative to a paraxial measurement (accommodative lag) when the eyes are accommodating, whereas in the unaccommodated state the minRMS measurement of refractive state may still be myopic relative to a paraxial refraction.[42] In the presence of large aberrations characteristic of zonal multifocal optics, estimates of SER are especially affected by the selected criterion for focus.[28] Additionally, the amplified contribution of off-axis optical aberrations[51] and the very obvious parallax shift of zones across the pupil associated with peripheral imaging all complicate the interpretation of any measure of peripheral refractive state.[29] To minimise these complicating issues, we employed a zone-specific analysis of refractive state, centred at the CL centre, concentrating on the pupil regions covered by the DF CL centre and first annular zones (*Figures 2* and *5*). This approach, however, has some potential limitations. In order to compare accommodative behaviour with the SV CLs, we assumed that the SV and DF CLs position similarly on the eye, which likely is an approximation.[52] Also, our zone-specific analysis approach evaluated only the mean power within each zone, whereas in reality power will vary within the zone, but by much less than the power varies across the whole pupil.

In the poor accommodating group, refractive states for the region of the pupil covered by the first CL annular zone showed a shift from myopic to hyperopic defocus at the largest measured eccentricity (30° temporal retina/nasal field at −4.00 D target vergence; *Figure 5*). Similar observation of hyperopic shifts at 40° eccentricity has been reported with two bifocal CLs in a simulation study.[29] This shift is believed to be attributed to the complicated interaction of CL decentration, eye-plus-lens aberrations (e.g., astigmatism, coma and other high order aberrations) and eye shape.[53]

The zone-specific analysis (*Figure 5*) and the pupil proportion analyses (*Figures 6*, *7* and *8*) both show that DF CLs successfully provided a majority of myopic defocus for the good accommodating participants in this study at all viewing distances, in spite of increased negative spherical aberration at near. For most tested conditions, the DF CL even successfully prevented hyperopic defocus from becoming dominant in the poor accommodating participants. This result indicates that even individuals with higher accommodative lags may still be treated effectively with MiSight 1 day DF zonal CLs containing +2.00 D defocus, but they might experience more benefit from an optical design with a higher defocus. Although the successful introduction of myopic defocus in young adult myopes even in the presence of significant accommodative lag is clearly shown here, it is important that these experiments be replicated in children who are undergoing myopia progression and myopia treatment. Collectively, these results also indicate potential clinical utility in measuring accommodative lag, pupil size and ocular aberrations when implementing myopia control treatment.

ACKNOWLEDGMENTS

The authors thank Professor Arthur Bradley, and Drs. Eric Seemiller, Olivia Reed, Viswanathan Ramasubramanian and Javier Gantes for their help with this project.

CONFLICT OF INTEREST

None.

AUTHOR CONTRIBUTIONS

Neeraj K Singh: Conceptualization (equal); Data curation (equal); Formal analysis (lead); Investigation (lead); Methodology (lead); Project administration (equal); Resources (equal); Software (equal); Supervision (equal); Validation (equal); Visualization (equal); Writing-original draft (lead); Writing-review & editing (lead). **Dawn Meyer:** Conceptualization (equal); Data curation (equal); Formal analysis (equal); Investigation (equal); Methodology (equal); Project administration (equal); Resources (equal); Supervision (equal); Validation (equal); Visualization (equal); Writing-original draft (equal); Writing-review & editing (equal). **Matt Jaskulski:** Conceptualization (equal); Data curation (equal); Formal analysis (equal); Methodology (equal); Resources (equal); Software (equal); Validation (equal); Writing-original draft (equal); Writing-review & editing (equal). **Pete Kollbaum:** Conceptualization (equal); Data curation (equal); Formal analysis (equal); Funding acquisition (lead); Investigation (equal); Methodology (equal); Project administration (lead); Resources (equal); Software (equal); Supervision (lead); Validation (equal); Visualization (equal); Writing-original draft (equal); Writing-review & editing (equal).

ORCID

Neeraj K Singh https://orcid.org/0000-0003-3424-3492
Dawn Meyer https://orcid.org/0000-0002-5157-2557
Matt Jaskulski https://orcid.org/0000-0001-5824-7135
Pete Kollbaum https://orcid.org/0000-0001-9568-2064

REFERENCES

1. Smith EL 3rd. Optical treatment strategies to slow myopia progression: effects of the visual extent of the optical treatment zone. *Exp Eye Res* 2013;114:77–88.
2. Mutti DO. To emmetropize or not to emmetropize? The question for hyperopic development. *Optom Vis Sci* 2007;84:97–102.
3. Rempt F, Hoogerheide J, Hoogenboom WP. Peripheral retinoscopy and the skiagram. *Ophthalmologica* 1971;162:1–10.
4. Smith EL 3rd, Hung LF, Huang J. Relative peripheral hyperopic defocus alters central refractive development in infant monkeys. *Vision Res* 2009;49:2386–2392.
5. Smith EL 3rd, Hung LF. The role of optical defocus in regulating refractive development in infant monkeys. *Vision Res* 1999;39:1415–1435.
6. Smith EL 3rd, Hung LF, Huang J, Arumugam B. Effects of local myopic defocus on refractive development in monkeys. *Optom Vis Sci* 2013;90:1176–1186.
7. Mutti DO, Hayes JR, Mitchell GL, *et al*. Refractive error, axial length, and relative peripheral refractive error before and after the onset of myopia. *Invest Ophthalmol Vis Sci* 2007;48:2510–2519.
8. Gwiazda J, Thorn F, Bauer J, Held R. Myopic children show insufficient accommodative response to blur. *Invest Ophthalmol Vis Sci* 1993;34:690–694.
9. Mutti DO, Mitchell GL, Hayes JR, *et al*. Accommodative lag before and after the onset of myopia. *Invest Ophthalmol Vis Sci* 2006;47:837–846.
10. Fincham EF. The mechanism of accommodation. London: G. Pulman & Sons; 1937.
11. Kabali HK, Irigoyen MM, Nunez-Davis R, *et al*. Exposure and use of mobile media devices by young children. *Pediatrics* 2015;136:1044–1050.
12. Lanca C, Saw S-M. The association between digital screen time and myopia: a systematic review. *Ophthalmic Physiol Opt* 2020;40:216–229.
13. Singh NK. Letter to the editor: myopia epidemic post-coronavirus disease 2019. *Optom Vis Sci* 2020;97:911–912.
14. Singh NK, James RM, Yadav A, *et al*. Prevalence of myopia and associated risk factors in schoolchildren in north India. *Optom Vis Sci* 2019;96:200–205.
15. Wallman J, Winawer J. Homeostasis of eye growth and the question of myopia. *Neuron* 2004;43:447–468.
16. Chamberlain P, Peixoto-de-Matos SC, Logan NS, *et al*. A 3-year randomized clinical trial of misight lenses for myopia control. *Optom Vis Sci* 2019;96:556–567.
17. Walline JJ, Greiner KL, McVey ME, Jones-Jordan LA. Multifocal contact lens myopia control. *Optom Vis Sci* 2013;90:1207–1214.
18. Altoaimi BH, Kollbaum P, Meyer D, Bradley A. Experimental investigation of accommodation in eyes fit with multifocal contact lenses using a clinical auto-refractor. *Ophthalmic Physiol Opt* 2018;38:152–163.
19. Flitcroft DI, He M, Jonas JB, *et al*. IMI – defining and classifying myopia: a proposed set of standards for clinical and epidemiologic studies. *Invest Ophthalmol Vis Sci* 2019;60:M20–M30.
20. Kollbaum P, Jansen M, Thibos L, Bradley A. Validation of an off-eye contact lens shack-hartmann wavefront aberrometer. *Optom Vis Sci* 2008;85:E817–E828.
21. Kollbaum PS, Jansen ME, Tan J, Meyer DM, Rickert ME. Vision performance with a contact lens designed to slow myopia progression. *Optom Vis Sci* 2013;90:205–214.
22. Singh NK, Jaskulski M, Ramasubramanian V, *et al*. Validation of a clinical aberrometer using pyramidal wavefront sensing. *Optom Vis Sci* 2019;96:733–744.
23. Jaskulski M, Singh NK, Bradley A, Kollbaum PS. Optical and imaging properties of a novel multi-segment spectacle lens designed to slow myopia progression. *Ophthalmic Physiol Opt* 2020;40:549–556.
24. Mathur A, Atchison DA. Peripheral refraction patterns out to large field angles. *Optom Vis Sci* 2013;90:140–147.
25. Wei X, Thibos LN. Modal estimation of wavefront phase from slopes over elliptical pupils. *Optom Vis Sci* 2010;87:E767–E777.
26. Southwell WH. Wave-front estimation from wave-front slope measurements. *J Opt Soc Am* 1980;70:998–1006.
27. Xu R, Bradley A, Lopez Gil N, Thibos LN. Modelling the effects of secondary spherical aberration on refractive error, image quality and depth of focus. *Ophthalmic Physiol Opt* 2015;35:28–38.
28. Campbell CE. Determining spherocylindrical correction using four different wavefront error analysis methods: comparison to manifest refraction. *J Refract Surg* 2010;26:881–890.
29. Ji Q, Yoo YS, Alam H, Yoon G. Through-focus optical characteristics of monofocal and bifocal soft contact lenses across the peripheral visual field. *Ophthalmic Physiol Opt* 2018;38:326–336.
30. Almutleb ES, Bradley A, Jedlicka J, Hassan SE. Simulation of a central scotoma using contact lenses with an opaque centre. *Ophthalmic Physiol Opt* 2018;38:76–87.
31. Jaisankar D, Leube A, Gifford KL, Schmid KL, Atchison DA. Effects of eye rotation and contact lens decentration on horizontal peripheral refraction. *Ophthalmic Physiol Opt* 2019;39:370–377.
32. Wang YZ, Thibos LN, Bradley A. Effects of refractive error on detection acuity and resolution acuity in peripheral vision. *Invest Ophthalmol Vis Sci* 1997;38:2134–2143.
33. Guirao A, Artal P. Off-axis monochromatic aberrations estimated from double pass measurements in the human eye. *Vision Res* 1999;39:207–217.
34. Lopez-Gil N, Fernandez-Sanchez V. The change of spherical aberration during accommodation and its effect on the accommodation response. *J Vis* 2010;10:12. doi.org/10.1167/10.13.12
35. Plainis S, Ginis HS, Pallikaris A. The effect of ocular aberrations on steady-state errors of accommodative response. *J Vis* 2005;5:466–477.
36. Bradley A, Nam J, Xu R, Harman L, Thibos L. Impact of contact lens zone geometry and ocular optics on bifocal retinal image quality. *Ophthalmic Physiol Opt* 2014;34:331–345.
37. Leat SJ. To prescribe or not to prescribe? Guidelines for spectacle prescribing in infants and children. *Clin Exp Optom* 2011;94:514–527.
38. Miller JM, Harvey EM. Spectacle prescribing recommendations of aapos members. *J Pediatr Ophthalmol Strabismus* 1998;35:51–52.
39. Altoaimi BH, Almutairi MS, Kollbaum PS, Bradley A. Accommodative behavior of young eyes wearing multifocal contact lenses. *Optom Vis Sci* 2018;95:416–427.
40. Madrid-Costa D, Ruiz-Alcocer J, Radhakrishnan H, Ferrer-Blasco T, Montes-Mico R. Changes in accommodative responses with multifocal contact lenses: a pilot study. *Optom Vis Sci* 2011;88:1309–1316.
41. Ruiz-Alcocer J, Madrid-Costa D, Radhakrishnan H, Ferrer-Blasco T, Montes-Mico R. Changes in accommodation and ocular aberration with simultaneous vision multifocal contact lenses. *Eye Contact Lens* 2012;38:288–294.
42. Thibos LN, Bradley A, Lopez-Gil N. Modelling the impact of spherical aberration on accommodation. *Ophthalmic Physiol Opt* 2013;33:482–496.
43. Calver R, Radhakrishnan H, Osuobeni E, O'Leary D. Peripheral refraction for distance and near vision in emmetropes and myopes. *Ophthalmic Physiol Opt* 2007;27:584–593.
44. Davies LN, Mallen EA. Influence of accommodation and refractive status on the peripheral refractive profile. *Br J Ophthalmol* 2009;93:1186–1190.
45. Lundstrom L, Mira-Agudelo A, Artal P. Peripheral optical errors and their change with accommodation differ between emmetropic and myopic eyes. *J Vis* 2009;9:17. doi.org/10.1167/9.6.17

46. Smith G, Millodot M, McBrien N. The effect of accommodation on oblique astigmatism and field curvature of the human eye. *Clin Exp Optom* 1988;71:119–125.
47. Whatham A, Zimmermann F, Martinez A, *et al*. Influence of accommodation on off-axis refractive errors in myopic eyes. *J Vis* 2009;9:11–13.
48. Berntsen DA, Kramer CE. Peripheral defocus with spherical and multifocal soft contact lenses. *Optom Vis Sci* 2013;90:1215–1224.
49. Jaisankar D, Liu Y, Kollbaum P, *et al*. Nasal-temporal asymmetry in peripheral refraction with an aspheric myopia control contact lens. *Biomed Opt Express* 2020;11:7376–7394.
50. Walker TW, Mutti DO. The effect of accommodation on ocular shape. *Optom Vis Sci* 2002;79:424–430.
51. Wang YZ, Thibos LN. Oblique (off-axis) astigmatism of the reduced schematic eye with elliptical refracting surface. *Optom Vis Sci* 1997;74:557–562.
52. Kollbaum PS Optical aberrations of contact lenses and eyes corrected with contact lenses. PhD Thesis, Indiana University; 2007.
53. Atchison DA, Rosen R. The possible role of peripheral refraction in development of myopia. *Optom Vis Sci* 2016;93:1042–1044.

How to cite this article: Singh NK, Meyer D, Jaskulski M, Kollbaum P. Retinal defocus in myopes wearing dual-focus zonal contact lenses. *Ophthalmic Physiol Opt* 2022;42:8–18. doi: 10.1111/opo.12903